Pt/Si-MCM-41 介孔结构对低温 NO+H₂+O₂ 反应的影响

武　鹏　　刘运霞　　章福祥　　李兰冬　　杨雅莉　　关乃佳*

(南开大学化学学院新催化材料研究所, 天津　300071)

摘要：　将 Pt/Si-MCM-41 用于 H₂ 选择催化还原(H₂-SCR)消除 NO 的反应. X 射线衍射分析、N₂ 吸附/脱附、氢吸附和透射电镜等分析结果表明, 介孔 Si-MCM-41 具有大的比表面积和孔体积有利于活性组分 Pt 的分散, Pt/Si-MCM-41 催化剂在富氧和 80000 h⁻¹ 空速的条件下, 其 H₂-SCR 低温活性在 100 ℃达到 60.1%, 优于 Pt/Si-ZSM-5 和 Pt/SiO₂ 催化剂, 其选择性在 120 ℃可达 70%. 当 Si-MCM-41 的介孔结构被破坏时, H₂-SCR 反应活性明显下降, 最大活性在 120 ℃仅为 15%. 漫反射红外光谱(DRIFTS)测试表明, —NO₃ 物种是 Pt/Si-MCM-41 催化剂在 H₂-SCR 反应中的主要中间物种.

关键词：　H₂-SCR；　NO；　富氧；　Si-MCM-41；　低温；　DRIFTS

中图分类号：　O647；　O643

Influences of Mesoporous Structure on the NO+H₂+O₂ Low Temperature Reaction over Pt/Si-MCM-41 Catalyst

WU Peng　　LIU Yun-Xia　　ZHANG Fu-Xiang　　LI Lan-Dong　　YANG Ya-Li　　GUAN Nai-Jia*

(*Institute of New Catalytic Materials Science, College of Chemistry, Nankai University, Tianjin　300071, P. R. China*)

Abstract：　It was found that Si-MCM-41 mesoporous molecular sieves as a support of noble metal Pt could be used for the selective catalytic reduction of NO by hydrogen (H₂-SCR) under lean-burn conditions. Pt/Si-MCM-41, together with Pt/Si-ZSM-5 and Pt/SiO₂, was characterized by X-ray diffraction analysis (XRD), nitrogen adsorption/desorption, hydrogen adsorption, and transmission electron microscopy (TEM). The results indicated that Pt/Si-MCM-41 had the best H₂-SCR activity in comparison with Pt/Si-ZSM-5 and Pt/SiO₂ catalysts and that the maximum conversion of NO was up to 60.1% at 100 ℃ and a gas hourly space velocity (GHSV) of 80000 h⁻¹ under lean-burn conditions. Characterization showed that the large surface area and pore volume of MCM-41 favored the dispersion of Pt. The maximum NO conversion of Pt/Si-MCM-41 catalyst decreased obviously to 15% at 120 ℃ when the pore structure of Si-MCM-41 support was destroyed. The reaction mechanism over Pt/Si-MCM-41 was investigated using *in situ* diffuse reflectance infrared spectroscopy (DRIFTS), which revealed that the main reaction intermediates should be nitrate species during NO reduction.

Key Words：　H₂-SCR；　NO；　Excess oxygen；　Si-MCM-41；　Low temperature；　DRIFTS

Nitrogen oxides (NO, NO₂, and N₂O), released from both mobile and stationary sources, are major air pollutants that greatly contribute to the formation of photochemical smog, acid rain, ozone depletion, ground-level ozone, and greenhouse effects[1]. Developed for several decades, three-way catalysts (TWCs) have been successfully commercialized; however, a fatal shortcoming is their failure to remove NOₓ at low temperature or under lean conditions. Therefore, there is an urgent need to develop a new catalytic system for operation under such conditions. At present, the commercially available technology for reducing NOₓ (x=1, 2) emissions from stationary sources is selective catalytic reduction of NOₓ by NH₃ (NH₃-SCR), while hydrocarbons as re-

ducing agents have been extensively studied according to recent reviews[2–5]. It was suggested that NH_3 was not an exclusive reducing agent for the catalytic removal of NO_x under lean-burn conditions.

The long-term prospects of hydrogen (fueling internal combustion engines, fuel cell vehicles, on-board reforming of diesel fuel, producing essentially only water vapor), as an environmentally benign agent, make hydrogen the most likely candidate as a reductant in a SCR reaction to abate NO_x emissions in an excess oxygen environment, such as diesel engine exhaust. Recently, much attention has been paid to the selective catalytic reduction of NO by hydrogen (H_2-SCR) due to higher activity and increasing N_2 formation at low temperatures[6–12]. Yokota *et al.*[6] reported that an improved catalyst of Pt-Mo-Na/SiO_2 had a wider temperature window for NO conversion and a more selectivity to N_2 than the conventional Pt catalysts. Burch and Coleman[7] found the Pt/SiO_2 catalysts to be more active at lower temperatures than the Pt/Al_2O_3 catalysts in de-NO_x reduction with H_2 under lean-burn condition. Costa *et al.*[8] believed the oxygen vacancies over Pt/$La_{0.5}Ce_{0.5}MnO_3$ were thought to participate in the mechanism of SCR and observed higher NO activity and N_2 selectivity. Other supports, such as zeolite[9,10], TiO_2-ZrO_2[11], MgO-CeO_2[12], Mg-Al-O[13], and $Sn_{0.9}In_{0.1}P_2O_7$[14] are also reported to be effective. Among these catalysts, platinum-based catalysts have been found to be the most active ones for the NO+H_2+O_2 reaction in an excess O_2 at low temperatures (T<200 ℃); however, their activities depend on the properties of support materials[5–15]. Therefore, this effect draws our attention to investigate the use of other materials as catalyst supports for NO reduction by Pt catalysts. MCM-41, a novel silica material discovered by Kresge *et al.* [16], has a mesoporous structure with regular arrangement of hexagonal channels and large pore volume, wherein the pore size can be varied between 0.2 and 10.0 nm and allows for a potentially high dispersion of active sites for catalysis. The advantages of MCM-41 have attracted considerable interests for the application of MCM-41 as a catalyst or a catalyst support[17–20]. The properties of MCM-41 as a catalyst support demonstrate the potential abilities to attain high reaction activity and reaction rate with diffusion of gases. Long and Yang[21] discovered the highest specific reaction rate for selective catalytic reduction of NO by hydrocarbons over Pt/MCM-41 compared with other ordinary catalyst supports. Although the novel type of mesoporous catalyst attracts great interests to the application in HC-SCR of NO and its catalytic performance has been widely studied[22–24], in this article, Pt/Si-MCM-41 was used for NO reduction of H_2-SCR. Considering Pt′s superior low temperature reduction capability, it was used as the active component on Si-MCM-41 support because H_2-SCR is usually performed at low temperature.

In this article, H_2-SCR of NO over Pt/Si-MCM-41 has been carried out first. The effects of silica structure and pore size of the silica supports were investigated in terms of catalytic activity in H_2-SCR under excess oxygen conditions at a gas hourly space velocity (GHSV) of 80000 h^{-1}. It indicated that the mesoporous structure of Pt/Si-MCM-41 could improve H_2-SCR activity under excess oxygen condition at a GHSV of 80000 h^{-1}. These results provided useful information on the role of support porosity and on the type of silica during the de-NO_x process, with hydrogen under lean-burn conditions on the supported platinum catalysts.

During the H_2-SCR on Pt/Si-MCM-41, the appearance and disappearance of various surface species were recorded by *in situ* diffuse reflectance infrared spectroscopy (DRIFTS) to obtain additional information on the reaction mechanism.

1 Experimental

1.1 Synthesis of catalysts

The pure siliceous SiO_2, Si-MCM-41, and Si-ZSM-5 supports were supplied by Nanlian Research Institution and the Catalysts Plant of Nankai University (China), respectively. Pt(1%, mass fraction, *w*) catalysts were prepared by incipient wetness impregnation method, using potassium chloroplatinate as the platinum precursor. The catalysts were dried at 100 ℃ and calcined in air at 500 ℃ for 3 h. Si-MCM-41 was treated with steam at 600 ℃ for 5 h and defined as Si-MCM-41 *.

1.2 Methods

The SCR reaction of NO by hydrogen at atmospheric pressure was carried out in a fixed-bed flow microreactor. The typical reactant gas mixture consists of NO (0.1% (volume fraction, φ)), H_2 (0.5% (φ)), and O_2 (6.7% (φ)), balanced with He to 100% (φ). The total flow rate of the inlet gas was set at 200 mL·min^{-1} and 0.05 g catalyst was used to obtain a GHSV of ca 80000 h^{-1}. The catalyst sample was initially treated at 500 ℃ in 93.3% (φ) He and 6.7% (φ) O_2 for 1 h before reactant gas mixture was introduced into the reactor. The products were analyzed online using a gas chromatograph (HP 6820 series) equipped with a TCD detector. A molecular sieve 5A column served for separation of N_2 and O_2, and a Porapak Q column for separation of N_2O. NO was analyzed by a chemiluminescence NO analyzer (AUTO5-1).

XRD analysis of the as-synthesized samples was performed on a Rigaku D/max 2500 diffractometer, equipped with a graphite monochromator and using Cu K_α radiation. The surface areas and pore properties of the samples were analyzed by nitrogen physisorption at 77 K using an adsorption porosimeter (TriStar 3000).

Before measurements were made, the sample was heated at 300 ℃ under vacuum for 2 h. A Brucker LEO1530VP scanning electron microscope (SEM) was used for studies of external surface morphology of samples. TEM was carried out with a PHILPS EM400ST TEM instrument.

In situ DRIFTS results were recorded on a Bruker Tensor 27-FTIR, equipped with a liquid N_2 cooled high sensitivity MCT detector. The samples for this study were well ground and placed in a ceramic crucible in an *in situ* chamber. Prior to each experiment, the samples were heated in He flow at 400 ℃ for 1 h, and then cooled to the desired temperature for obtaining a background spectrum. All gas mixtures were fed at a flow rate
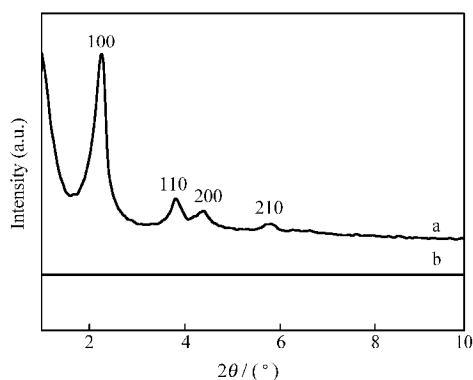
Fig.1　XRD patterns of supports
a) Si-MCM-41, b) Si-MCM-41 *

Table 1　Specific surface areas, pore volumes, and pore diameters of different supports

Support	$S_{BET}/(m^2 \cdot g^{-1})$	Pore volume $(cm^3 \cdot g^{-1})$	Pore diameter (nm)
Si-MCM-41	1267	0.96	2.7
Si-ZSM-5	377	0.16	0.055
SiO₂	180	–	–
Si-MCM-41 *	299	–	–

of 30 mL·min⁻¹. All spectra were measured with a resolution of 4 cm⁻¹ and with an accumulation of 100 scans. TPDRO 1100 was used to measure the Pt dispersion of catalysts by H₂ chemisorption at 30 ℃. Prior to analysis, the sample was reduced in H₂ at 500 ℃ for 1 h. The monolayer chemisorbed volume (V_m) was obtained based on the H₂ adsorption isotherm and extrapolation to p=0. The Pt dispersion was calculated from V_m by assuming molar ratio of $n_{Pt}:n_{H_2}$=2.

2　Results and discussion

Fig.1 shows the XRD patterns of the Si-MCM-41 samples, from which the formation of mesoporous structure of Si-MCM-41 materials can be demonstrated. An intensive peak observed at 2θ=2.3° corresponds to the (100) diffraction of the Si-MCM-41 framework. The other three reflection peaks can be attributed to crystal-free (110), (200), and (210) reflections of Si-MCM-41. On comparison, the sample Si-MCM-41 * with steam treatment at 600 ℃ did not show any peak from 1° to 10°, indicating the complete destruction of the mesoporous structure of Si-MCM-41. Conventional patterns of XRD, which represented Si-ZSM-5 and SiO₂, have been obtained.

The chemical properties of Si-ZSM-5, SiO₂, and Si-MCM-41 are quite similar[24] in the sense that they all do not contain framework Al. But as a support, some physical properties may be very important for catalytic performance, especially porous structure, surface area, etc. The average pore diameters calculated from N₂ adsorption isotherms using BJH model[25], the BET surface areas, and the pore volumes of the samples are presented in Table 1. The Si-MCM-41 showed much narrower pore-size distribution,

with size close to 2.7 nm; larger BET surface area (> 1000 m²· g⁻¹); and pore volume (close to 1.00 cm³·g⁻¹) with respect to SiO₂, Si-ZSM-5, and Si-MCM-41 *. Generally, the larger surface area of Si-MCM-41 will be beneficial to Pt dispersion[24], and its larger pore volume is favorable to the diffusion of reactant and product gases. The results proved that Pt dispersion on Pt/Si-MCM-41 reached 33.7%, whereas it was 18.9% and 17.4% for 1% (*w*) Pt/Si-ZSM-5 and 1% (*w*) Pt/SiO₂, respectively. Meantime, TEM images of freshly prepared catalysts are demonstrated in Fig.2. They also provided evidences, in which well-dispersed platinum clusters or nanoparticles in the pores of Si-MCM-41 smaller (< 2 nm) than the fringe width (3.5 nm) were not observed, suggesting a uniform distribution of platinum sites in the pore.

As shown in Fig.3, the SEM micrographs of the samples are different. The size of Si-ZSM-5 with common benzene-like particles is not very unique. The Si-MCM-41 exhibits completely different long-range disorder structures, compared with amorphous crystal of SiO₂. It is also noticed that the sample of steamed Si-MCM-41 * (Fig.3d) shows an aggregation without regular shape and size compared with untreated sample (Fig.3c).

From the TEM images of Si-MCM-41 samples before and after steam treatment (Fig.4), it can be concluded that the morphologies of the samples are not identical. Regular mesoporous structures with hexagonal channel arrays can be observed clearly on the Si-MCM-41 sample. However, as seen with steamed Si-MCM-41 * in Fig.4a, no well-defined hexagonal structure and channels were detected, indicating that the hexagonal mesoporous structure had mostly collapsed, well-supported by the observation of XRD results.

Table 2 gives the NO conversion in H₂-SCR on the catalysts of the different supports for Pt at several typical reaction temperatures ranging from 60 to 260 ℃. It showed that the maximum NO conversion reached only 31.5% at 160 ℃ over 1% (*w*) Pt/SiO₂, whereas it was 42.8% at 120 ℃ over 1% (*w*) Pt/Si-ZSM-5; in contrast to this, the NO conversion of 60.1% at 100 ℃ on
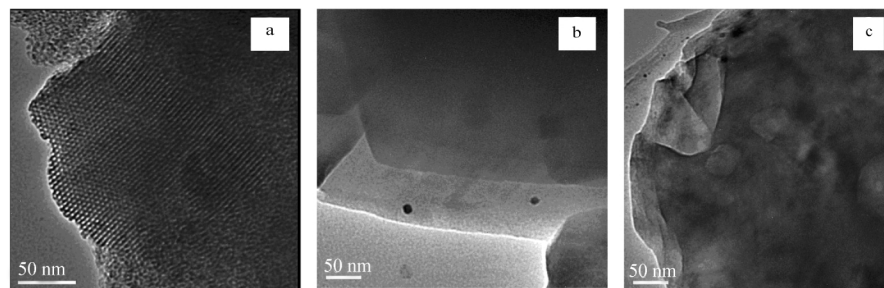

Fig.2　TEM images of different catalysts
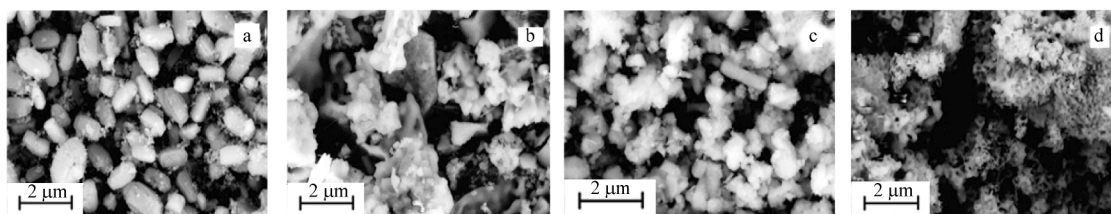(a) 1% (*w*) Pt/Si-MCM-41, (b) 1% (*w*) Pt/Si-ZSM-5, (c) 1% (*w*) Pt/SiO₂

Fig.3   SEM images of different supports

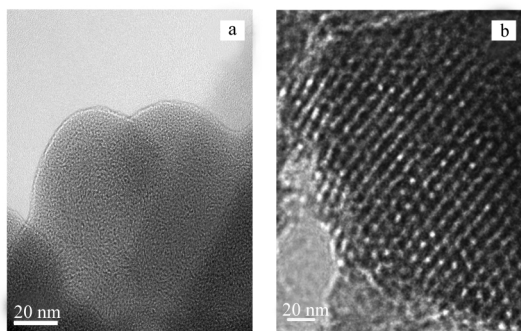(a) Si-ZSM-5, (b) SiO$_2$, (c) Si-MCM-41, (d) Si-MCM-41 *

Fig.4   TEM images of the untreated and treated Si-MCM-41 samples
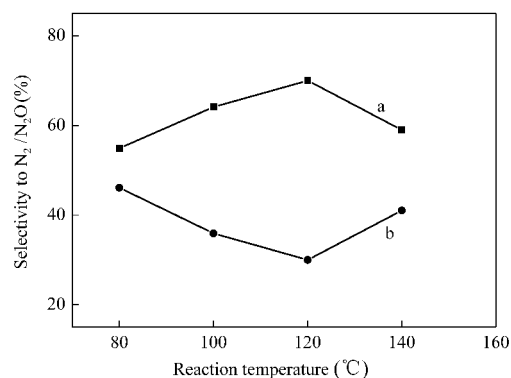
(a) Si-MCM-41 *, (b) Si-MCM-41

Fig.5   Selectivities to N$_2$/N$_2$O over 1% (w) Pt/Si-MCM-41 catalysts

(a) selectivity to N$_2$, (b) selectivity to N$_2$O;

The feed compositions are the same as those in Table 2.

1% (w) Pt/Si-MCM-41 has been obtained. This reveals that Pt/Si-MCM-41 has higher NO reduction activities and lower reaction temperature than Pt/SiO$_2$ and Pt/Si-ZSM-5 under the same reaction condition. Table 2 also shows that NO conversion over Pt/Si-MCM-41 increases significantly from 60 to 100 ℃, reaching a maximum at an optimal reaction temperature (T_m=100 ℃), and then decreases at elevated temperatures, which might be due to competing H$_2$-O$_2$ combustion reaction, in which H$_2$ was exhausted in non de-NO$_x$ process[11]. Compared with Pt/SiO$_2$ and Pt/Si-ZSM-5 catalysts, the better NO reduction activity on Pt/Si-MCM-41 might be attributed to high surface area and large pore volume of MCM-41. Meanwhile, the selectivity of the conversion of NO to N$_2$ on the Pt/Si-MCM-41 was also investigated (Fig.5) and the maximum selectivity to N$_2$ amounted to 70%. The supports of Si-ZSM-5, SiO$_2$, and Si-MCM-41 are individually grouped to microporous molecular sieves, amorphous crystals, and mesoporous structure, respectively. Therefore, the differences in NO conversion of H$_2$-SCR could be attributed to the pore-structure effects of the support.

In order to further verify the effects of mesoporous pore struc-

ture, a Pt/Si-MCM-41 * whose support was initially treated by water steam at 600 ℃ for 5 h and then loaded with 1% (w) Pt has been tested. As seen in Fig.6, the NO-H$_2$-O$_2$ reaction activity over Pt/Si-MCM-41 * was obviously much lower than that over Pt/Si-MCM-41. From the results of XRD, TEM, and BET, it was confirmed that the mesoporous pore structure of Si-MCM-41 has almost been destroyed. This indicates that the pore structure property of the Si-MCM-41 mesoporous materials plays an important role in the activity of NO reduction with hydrogen on platinum.

To determine the mechanism for the selective catalytic reduction of NO in the presence of excess oxygen over Pt/Si-MCM-41, the intermediates produced during H$_2$-SCR reaction were in-
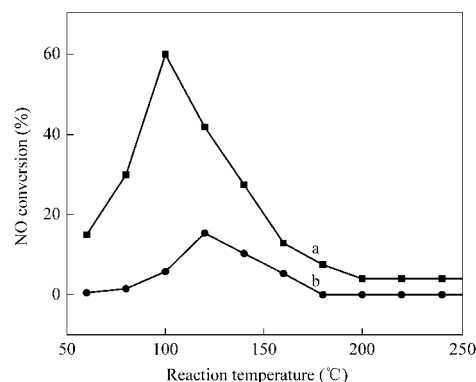
Table 2   NO conversion over 1% (w) Pt catalysts loaded on different supports

Catalyst	T/℃										
	60	80	100	120	140	160	180	200	220	240	260
	NO conversion (%)										
Pt/Si-MCM-41	15.0	30.0	60.1	41.9	27.5	12.9	7.5	4.0	4.0	4.0	10.0
Pt/SiO$_2$	0.7	4.1	9.9	19.0	28.4	31.5	23.3	20.7	16.6	5.0	0.0
Pt/Si-ZSM-5	0.0	25.0	33.8	42.8	30.0	1.6	0.0	0.0	0.0	0.0	0.0

feed compositions: H$_2$: 0.5% (φ), NO: 0.1% (φ), O$_2$: 6.7% (φ);

m: 0.05 g; GHSV: 80000 h^{-1}

Fig.6   Effect of the Si-MCM-41 mesoporous pore structure with 1% (w) Pt on NO conversion

(a) Pt/Si-MCM-41, (b) Pt/Si-MCM-41 *;

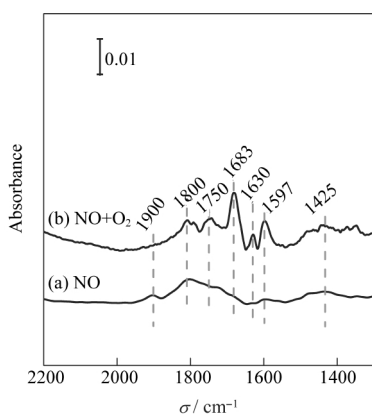The feed compositions are the same as those in Table 2.

Fig.7 *In situ* infrared spectra of Pt/Si-MCM-41 exposure to 0.1% (φ) NO (a) and 0.1% (φ) NO+ 6.7% (φ) O₂ (b) at 40 ℃ for 30 min

Fig.8 *In situ* infrared spectra of Pt/Si-MCM-41 exposure to 0.1% (φ) NO, 0.5% (φ) H₂, 6.7% (φ) O₂ and He as balance gas at different reaction temperatures for 30 min

vestigated using the *in situ* DRIFTS method. Fig.7 shows the *in situ* DRIFTS spectra of Pt/Si-MCM-41 recorded under different conditions at 40 ℃ for 30 min. After exposure to NO or NO+O₂ in He, the IR band at 1900 cm⁻¹ is attributed to the gas phase NO [26]. Three bands at 1800, 1750, and 1683 cm⁻¹ are observed on Pt/Si-MCM-41. These bands can be assigned to the nitrosyl species (—NO, —NO⁻, and —NO⁶⁺) adsorbed on Pt, respectively, which are in good agreement with those reported in the literature[26,27]. Two bands at 1630 and 1597 cm⁻¹ correspond to bidentate nitrates (—NO₃) adsorbed on the surface of Pt and the supports[28,29], which were formed when molecules were bridging two adjacent oxygen atoms. The IR band at 1425 cm⁻¹ is attributed to nitrito species(Pt-NO₂)[27]. As seen in Fig.7, no novel adsorbed species appeared after introduction of excess oxygen into the NO/He reaction system and only the peak intensities of all IR bands corresponding to nitrate species slightly increased. It could be clearly seen that O₂ will promote the formation of nitrates over Pt/Si-MCM-41.

DRIFTS study of the adsorbed species on Pt/Si-MCM-41 catalyst under reaction conditions (NO+H₂+O₂) at different temperatures, was also presented. As seen in Fig.8, the band at 1850 cm⁻¹ should be attributed to —NO adsorbed on catalyst[27]; no other difference in the adsorbed species at the temperature ranging from 80 to 200 ℃ under H₂-SCR conditions was found. In this case, only adsorbed inorganic N-containing (—NO, —NO₂, and —NO₃) species were observed during the reaction and these inorganic N-containing species might be responsible for NO reduction, in which the adsorbed nitrate species should be the most active ones to be reduced by gaseous hydrogen[28]. The intensities of bands corresponding to nitrate species decreased with increasing temperature and tended to slightly increase after 100 ℃. This trend was well in agreement with the change in NO conversion, and the adsorbed nitrate species were thought as the main reaction intermediates for NO reduction. Therefore, the hypothesis on the mechanism of NO reduction over Pt/Si-MCM-41 is suggested as follows[29]:
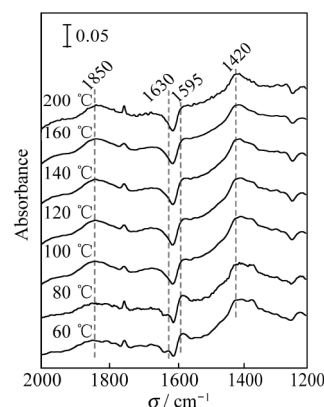
$$NO(g) \leftrightarrow NO(ad) \tag{1}$$

$$NO(ad)+O(ad) \rightarrow NO_2(ad) \tag{2}$$

$$NO_2(ad)+O(ad) \rightarrow NO_3(ad) \tag{3}$$

According to the FTIR results of Fig.8, the active intermediate nitrate species formed on Pt/Si-MCM-41 can react with the reductant H₂ to form the final products N₂, N₂O, and H₂O. Shen and Kawi[24,26] reported that the absorbance intensity and disappearance rate for the oxidation intermediates on 1% (*w*) Pt/Si-MCM-41 were much weaker than that on 1% (*w*) Pt/SiO₂, indicating that the reaction has been obviously affected by the different catalyst supports used because the loading of Pt was the same. In this article, from the FTIR results of Figs.7 and 8, it also indicated that the surface concentration of intermediates on Pt/Si-MCM-41 was low. This result implies that the mesoporous Si-MCM-41 support promotes the surface reaction between reaction intermediates and H₂ to form N₂ (or N₂O) or the decomposition of adsorbed reaction intermediates on account of the large surface of Si-MCM-41. As described in the literature, the low surface concentration of these reaction intermediates formed on Pt/Si-MCM-41 resulted in better activity for the removal of NO over Pt/Si-MCM-41 in H₂-SCR.

3　Conclusions

In this article, mesoporous support of Si-MCM-41 loaded by 1% (*w*) Pt was used in H₂-SCR. The results showed that this catalyst was active for the selective catalytic reduction of NO with hydrogen in the presence of excess oxygen. The maximum conversion of NO was 60.1% at 100 ℃ and GHSV of 80000 h⁻¹ under lean-burn conditions, superior to Pt/Si-ZSM-5 and Pt/SiO₂ catalysts. Conclusions have been drawn that the potential activity is mainly due to MCM-41 mesoporous material having high BET surface areas ($>$ 1000 m²·g⁻¹) and large pore volumes ($\approx$ 1.00 cm³·g⁻¹), which lead to well-dispersed active metal sites. NO conversion is dramatically decreased when the hexagonal mesoporous structure of MCM-41 has collapsed *via* results of XRD, TEM, and BET, which proved that NO activity should be closely related to the pore structure of the supports. In this case, —NO₃ species as the reaction intermediate played a very impor-

tant role in the selective catalytic reduction of NO by H_2 in the presence of excess oxygen by means of DRIFTS. However, the detailed reaction mechanism for the whole H_2-SCR was very complicated. The whole reaction network and main reaction pathways still need to be investigated further.

References

1   Seinfeld, J. H. *Science,* **1989, 243**: 745.

2   Fritz, A.; Pitchon, V. *Appl. Catal. B,* **1997, 13**: 1

3   Parvulescu, V. I.; Grange, P.; Delmon, B. *Catal. Today,* **1998, 46**: 233

4   Busca, G.; Lietti, L.; Ramis, G.; Berti, F. *Appl. Catal. B,* **1998, 18**: 1

5   Fang, H.; Cai, L.; Liu, P.; Zhao, M.; Zhang, L. J.; Gong, M. C.; Chen, Y. Q. *Acta Phys. -Chim. Sin.,* **2006, 22**(8): 1004 [房　华, 蔡　黎, 刘　萍, 赵　明, 张丽娟, 龚茂初, 陈耀强. 物理化学学报, **2006, 22**(8): 1004]

6   Yokota, K.; Fukui, M.; Tanaka, T. *Appl. Surf. Sci.,* **1997, 121/122**: 273

7   Burch, R.; Coleman, M. D. *Appl. Catal. B,* **1999, 23**: 115

8   Costa, C. N.; Stathopoulos, V. N.; Belessi, V. C.; Efstathiou, A. M. *J. Catal.,* **2001, 197**: 350

9   Satsuma, A.; Hattori, T.; Yoshida, H.; Shimizu, K.; Hashimoto, M.; Shibata, J. *J. Phys. Chem. B,* **2004, 108**: 18327

10 Machida, M.; Watanabe, T. *Appl. Catal. B,* **2004, 52**: 281

11 Machida, M.; Ikeda, S.; Kurogi, D.; Kijima, T. *Appl. Catal. B,* **2001, 35**: 107

12 Costa, C. N.; Efstathiou, A. M. *Appl. Catal. B,* **2007, 72**: 240

13 Hamada, S.; Ikeue, K.; Machida, M. *Appl. Catal. B,* **2007, 71**: 1

14 Hibino, T.; Nagao, M.; Teranishi, S.; Yoshii, T.; Tomita, A. *J. Catal.,* **2007, 247**: 137

15 Machida, M.; Watanabe, T.; Ikeda, S.; Kijima, T. *Catal. Commun.,* **2002, 3**: 233

16 Kresge, C. T.; Leonowicz, M. E.; Roth, W. J.; Vartuli, J. C.; Beck, J. S. *Nature,* **1992, 359**: 710

17 Davies, L. J.; McMorn, P.; Bethell, D.; Page, P. C. B.; King, F.; Hancock, F. E.; Hutchings, G. J. *J. Catal.,* **2001, 198**: 319

18 Fujiyama, H.; Kohara, I.; Iwai, K.; Nishiyama, S.; Tsuruya, S.; Masai, M. *J. Catal.,* **1999, 188**: 417

19 Yao, N.; Pinckney, C.; Lim, S.; Pak, C.; Haller, G. L. *Microporous Mesoporous Mater.,* **2001, 44**: 377

20 Xia, Q. H.; Hidajat, K.; Kawi, S. *J. Catal.,* **2002, 209**: 433

21 Long, R. Q.; Yang, R. T. *Catal. Lett.,* **1998, 52**: 91

22 Jentys, A.; Schießer, W.; Vinek, H. *Chem. Commun.,* **1999**: 335

23 Schießer, W.; Vinek, H.; Jentys, A. *Catal. Lett.,* **1998, 56**: 89

24 Shen, S. C.; Kawi, S. *Appl. Catal. B,* **2003, 45**: 63

25 Gregg, S. J.; Sing, K. S. W. Adsorption, surface area and porosity. London: Academic Press, 1982: Chap. 4

26 Shen, S. C.; Kawi, S. *J. Catal.,* **2003, 213**: 241

27 Coata, C. N.; Efstathiou, A. M. *J. Phys. Chem. C,* **2007, 111**: 3010

28 Li, L. D.; Zhang, F. X.; Guan, N. J.; Richter, M.; Fricke, R. *Catal. Commun.,* **2007, 8**: 583

29 Costa, C. N.; Efstathiou, A. M. *J. Phys. Chem. B,* **2004, 108**: 2620